



**HAL**  
open science

## Evolution of Cu(In,Ga)Se<sub>2</sub> surfaces under water immersion monitored by X-ray photoelectron spectroscopy

Solène Béchu, Muriel Bouttemy, Jacky Vigneron, Daniel L. Lincot, Jean-François Guillemoles, A. Etcheberry

► **To cite this version:**

Solène Béchu, Muriel Bouttemy, Jacky Vigneron, Daniel L. Lincot, Jean-François Guillemoles, et al.. Evolution of Cu(In,Ga)Se<sub>2</sub> surfaces under water immersion monitored by X-ray photoelectron spectroscopy. *Surface and Interface Analysis*, 2020, ECASIA'19, 52 (12), pp.975-979. 10.1002/sia.6896 . hal-03109149

**HAL Id: hal-03109149**

**<https://hal.science/hal-03109149v1>**

Submitted on 3 Feb 2021

**HAL** is a multi-disciplinary open access archive for the deposit and dissemination of scientific research documents, whether they are published or not. The documents may come from teaching and research institutions in France or abroad, or from public or private research centers.

L'archive ouverte pluridisciplinaire **HAL**, est destinée au dépôt et à la diffusion de documents scientifiques de niveau recherche, publiés ou non, émanant des établissements d'enseignement et de recherche français ou étrangers, des laboratoires publics ou privés.

# 1 Evolution of Cu(In,Ga)Se<sub>2</sub> surfaces under water immersion monitored by X-Ray 2 Photoelectron Spectroscopy

3 Solène Béchu<sup>1\*</sup>, Muriel Bouttemy<sup>1</sup>, Jackie Vigneron<sup>1</sup>, Daniel Lincot<sup>2</sup>, Jean-François  
4 Guillemoles<sup>2</sup>, Arnaud Etcheberry<sup>1</sup>

5 1. Institut Lavoisier de Versailles (ILV), Université Paris-Saclay, CNRS-UVSQ, 45 av. des  
6 Etats-Unis, Versailles 78035, France.

7 2. CNRS-IPVF, 18 boulevard Thomas Gobert, 91120 Palaiseau, France.

## 8 Abstract

9 Cu(In,Ga)Se<sub>2</sub> absorbers were immersed in deionized water for different times and specific  
10 chemical evolutions were monitored thanks to X-Ray Photoemission Spectroscopy.  
11 Cu(In,Ga)Se<sub>2</sub> related dissolution products were studied in water through Induced Coupled  
12 Plasma Optical Emission Spectroscopy. From those analyses, specific surface network  
13 disorganization was observed, with Cu migration towards the surface, leading to different  
14 kinetics of oxidation and dissolution for each element that could be quantified.

## 15 1. Introduction

16 Understanding the ageing mechanism of solar absorbers is a key point for the future of the  
17 photovoltaic market. Regarding the Cu(In,Ga)Se<sub>2</sub> (CIGS) solar cells technology, which reaches  
18 efficiencies up to 23.4%,<sup>1</sup> one key parameter to control during ageing is interfaces. Very few  
19 studies report on the properties modifications of CIGS solar devices following pure water  
20 exposure. Theelen and al. demonstrated that, over water dipping, the chemical repartition of  
21 element drastically evolves, leading to strong modifications of electrical properties of CIGS  
22 solar cells.<sup>2</sup> They also studied the ageing of different layers (Al:ZnO, Mo) necessary to the  
23 device fabrication during water immersion.<sup>3,4</sup> However, to our knowledge, the chemical  
24 evolutions induced by water on CIGS surface were not systematically explored. Indeed,  
25 immersion in water asks the question of the surface chemical behavior in front of an infinite  
26 water reservoir but also raises interrogations about differences with air ageing with a high  
27 moisture level, which induces possible interactions with a very thin water film, more or less  
28 continuous.<sup>5,6</sup>

29 In the present study, X-Ray Photoemission Spectroscopy (XPS) is employed to follow the  
30 chemical evolution of CIGS surfaces during different water immersion times, as it can provide

31 the evolution of the chemical environment as well as a quantitative analysis of the surface  
32 composition. This last point is of primary importance in the case of CIGS **as it will influence**  
33 **the band alignment with the buffer layer and can be monitored** through two main ratios: the  
34 GGI ( $[\text{Ga}]/([\text{Ga}]+[\text{In}])$ ) and the CGI ( $[\text{Cu}]/([\text{Ga}]+[\text{In}])$ ).

35 In this paper, long time evolution during pure water immersion of CIGS surfaces is presented.  
36 Modifications of the initial free oxide reference surface is studied by a regular monitoring of  
37 chemical environments during 4 weeks, principally on the base of Augers lines comparison,  
38 whose features enable to more easily evidence oxidation states. The examination is completed  
39 by the corresponding key ratios determined with the associated photopeaks. Surfaces studied  
40 are either reference ones, *i.e.* **without** oxides or binary phases (such as elementary selenium,  
41  $\text{Se}^0$ ), thanks to chemical engineering or aged surfaces (strongly oxidized).<sup>7,8</sup>

## 42 **2. Methods and Experimental Setup**

### 43 *2.1. CIGS samples*

44 The CIGS samples were supplied by ZSW (Zentrum für Sonnenenergie- und Wasserstoff-  
45 Forschung, Germany).<sup>9</sup> CIGS was co-evaporated on Mo (600 nm)/glass (3 mm) substrates. The  
46 CIGS layers were provided with expected GGI bulk ratio close to 0.3, a CGI of 1.0 and a  
47 thickness of 2.1  $\mu\text{m}$ . Surfaces were prepared to eliminate any traces of oxides,<sup>7</sup>  $\text{Se}^0$  and side  
48 phases.<sup>8</sup> The CIGS/water interaction was provided through immersion in 60 mL of ultra-pure  
49 de-ionized water (18.2 M $\Omega$ , without degassing **with a concentration of dissolved  $\text{O}_2$  of  $5.5 \pm$**   
50  **$0.6 \text{ mg L}^{-1}$** ) for several weeks. Experiments were performed in the dark.

### 51 *2.2. Experimental*

52 XPS surface chemical analyses were performed with a Thermo Electron K-Alpha<sup>+</sup> spectrometer  
53 using a monochromatic Al-K $\alpha$  X-Ray source (1486.6 eV). The X-Ray spot size was 400  $\mu\text{m}$ .  
54 High energy resolution spectra were acquired using a Constant Analyzer Energy (CAE) mode  
55 of 10 eV and 0.05 eV as energy step size. **X-Ray Auger Electron Spectroscopy (XAES)** lines  
56 were studied with a CAE mode of 50 eV and 0.1 energy step size. Data were processed using  
57 the Thermo Fisher scientific Avantage<sup>©</sup> data system with a Shirley-assimilated background  
58 subtraction and XPS compositions were deduced using the sensitivity factors, the transmission  
59 factor and inelastic mean-free paths from Avantage<sup>©</sup> library. The fits were performed with  
60 Gaussian/Lorentzian mix, determined on deoxidized samples. In this paper, ratios were  
61 calculated based on major photopeaks:  $\text{Ga}2p_{3/2}$ ,  $\text{Cu}2p_{3/2}$  and  $\text{In}3d_{5/2}$  and  $\text{Se}3d$ .

62 Dosages of Ga, In, Cu, Se and Na elements in water after different interaction times were  
63 performed by Induced Coupled Plasma Optical Emission Spectroscopy (ICP-OES) with an  
64 Agilent spectrometer. Calibrations were performed with set of standard solutions with a  
65 concentration range from 5 to 5000  $\mu\text{g L}^{-1}$  in  $\text{HNO}_3$  (4%).<sup>10</sup>

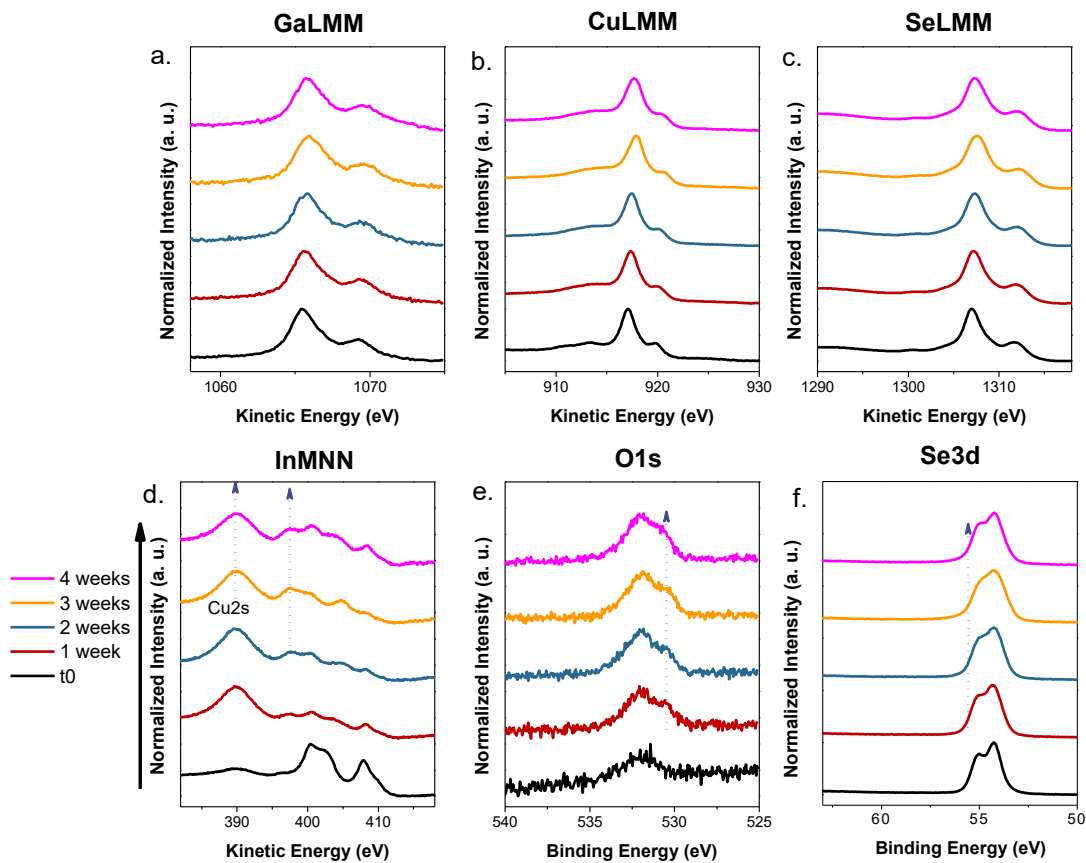
### 66 3. Results & Discussions

#### 67 3.1. Immersion of fresh CIGS surfaces

68 Regarding the chemical environment of fresh CIGS surface, for each constitutive element,  
69 initially only CIGS one is visible, either on the XAES lines (Figure 1,  $t_0$  spectra), or on the  
70 photopeaks. The Ga transition ( $\text{GaL}_3\text{M}_{45}\text{M}_{45}$ , Figure 1 a.,  $t_0$  spectrum) is representative of a sole  
71 CIGS environment at  $1065.7 \pm 0.1$  eV (Kinetic Energy, KE), without traces of Ga-O  
72 contribution ( $1062.5 \pm 0.1$  eV, KE). Similar behaviors are observed for Cu and Se transitions  
73 ( $\text{CuL}_3\text{M}_{45}\text{M}_{45}$  and  $\text{SeL}_3\text{M}_{45}\text{M}_{45}$ , Figure 1 b and c.,  $t_0$  spectra) positioned at  $917.2 \pm 0.1$  eV and  
74  $1307.2 \pm 0.1$  eV, KE respectively. The absence of oxide phases is supported by the fact that no  
75 shoulder is visible at lower KE ( $914.1 \pm 0.1$  eV) for Cu and no oxidized contribution at  $1300.6$   
76  $\pm 0.1$  eV, KE for Se. The Se3d photopeak (Figure 1 f.,  $t_0$  spectrum) is also presented here  
77 because of the large chemical shift due to Se-O bounds and clear distribution at low binding  
78 energy, with the  $\text{Se}^0$  contribution. A sole  $\text{Se}3\text{d}_{5/2}$  CIGS environment is observed at  $54.1 \pm 0.1$   
79 eV (Binding Energy, BE) and no oxide or  $\text{Se}^0$  contributions are observed ( $58.8 \pm 0.1$  and  $55.1$   
80  $\pm 0.1$  eV, BE respectively).<sup>11</sup> The  $\text{InM}_{4/5}\text{N}_{45}\text{N}_{45}$  X-Auger region without traces of oxides is  
81 presented in Figure 1 d. ( $t_0$  spectrum), with the main CIGS contribution at  $400.5 \pm 0.1$  eV, KE,  
82 while the In-O one should be located at  $398.6 \pm 0.1$  eV, KE. On this specific region, another  
83 photopeak is of primary importance, the Na1s one, at  $415.2 \pm 0.1$  eV, KE. Na is a key element  
84 to enhance CIGS performances.<sup>12</sup> In present soda-lime conventional configuration, Na migrates  
85 from the substrate to CIGS front side. On  $t_0$  spectrum, no Na traces are found thanks to  
86 deoxidation/cleaning process. Its reemergence and its associated kinetic can be found in  
87 literature.<sup>5,6</sup> Finally, the O1s photopeak region (540-525 eV, BE, Figure 1 e.) provides  
88 information about the inherent carboneous contamination ( $531.7 \pm 0.1$  eV, BE) but also on  
89 oxide phase ( $531.0 \pm 0.1$  eV, BE). For the  $t_0$  spectrum, only inherent contamination is visible.

90 To investigate the CIGS/pure water interaction evolutions, a dedicated experiment focused on  
91 the interactions between water and CIGS surfaces by immersing the absorber in infinite  
92 deionized water for 4 weeks. The sample was regularly extracted for XPS analysis and then  
93 replaced in the aqueous medium. Long-time interactions with water lead to non-expected

94 effects on CIGS surfaces. The first one concerns the Cu signal. Indeed, after one week of ageing,  
95 an important increase of Cu content is noted at the surface with a CGI value which triples (Table  
96 1) and consequently the emergence of a notable Cu<sub>2s</sub> photopeak ( $388.7 \pm 0.1$  eV KE, Figure 1  
97 d.) on the In-MNN Auger region. It is strengthened over times as shown by the increase of CGI  
98 ratio value (Table 1). Moreover, the Auger parameter varies from  $1849.4 \pm 0.1$  eV (typical of  
99 CIGS environment) to  $1850.0 \pm 0.1$  eV, showing a modification of the chemical environment  
100 of Cu over time, also supported by the FWHM evolution of the Cu 2p<sub>3/2</sub> photopeak which  
101 increases gradually from  $0.98 \pm 0.03$  to  $1.07 \pm 0.03$  eV after 4 weeks ageing. The second  
102 modification concerns the fast oxidation of In element, as observed with the appearance of In  
103 oxide contribution at  $398.5 \pm 0.1$  eV, KE (Figure 1 d.). This is accompanied with a decrease of  
104 the GGI ratio, which is divided by two after one-week ageing (Table 1). This modification of  
105 the surface content is due to important Cu migration upon the absorber, which is in contradiction  
106 with surfaces exposed to ambient atmosphere.<sup>6</sup> After the four weeks of ageing, an important  
107 surface degradation appears on samples, with a possible surface delaminating. Thus, the ageing  
108 procedure in pure water has been stopped, the representativeness of surface analyses being  
109 questionable.



110

111 **Figure 1: Normalized evolution of high energy XPS spectra of reference CIGS surface (HCl + KCN treated) over 4**  
 112 **weeks of water-ageing: GaLMM (a.), CuLMM (b.), SeLMM (c.), InMNN (d.) Auger regions and O1s (e.) and Se3d (f.)**  
 113 **photopeaks. The differences observed are represented with an arrow.**

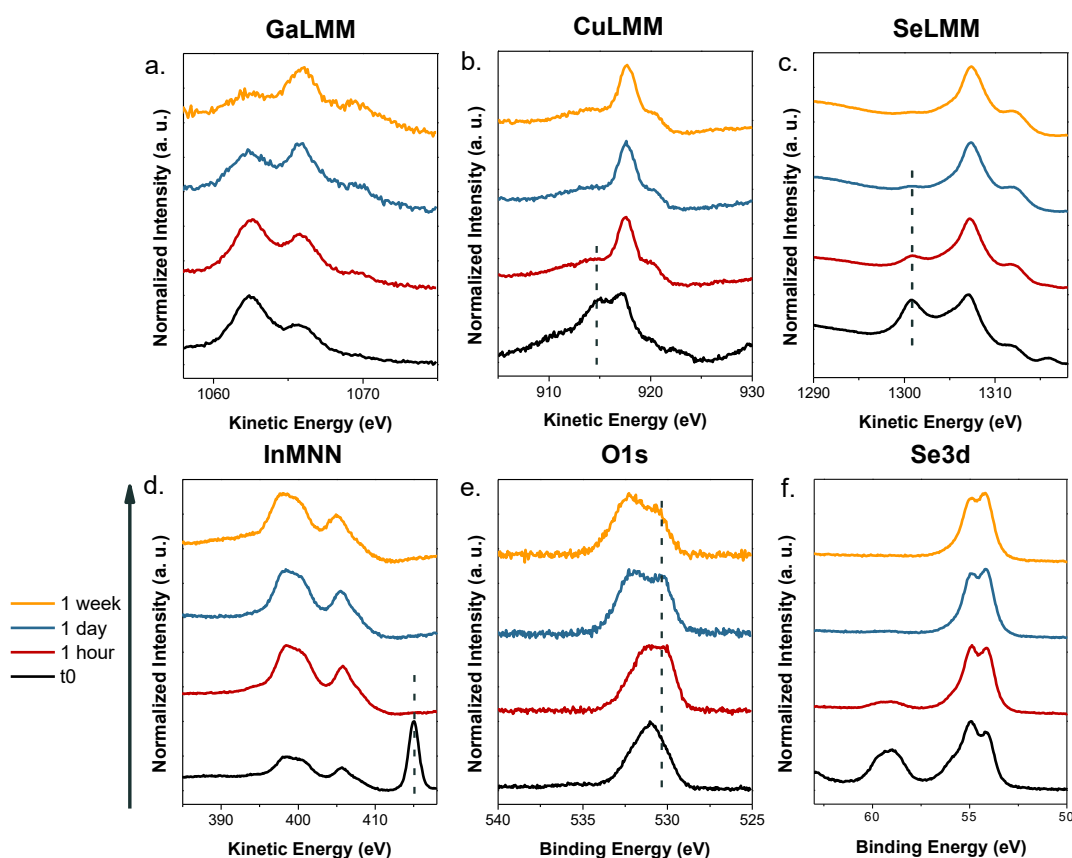
114

115 According to the In behavior over time, the possibility that the other elements of CIGS network  
 116 also oxidize in water is rather probable even if no traces of oxides are evidenced by surface  
 117 analyses. The explanation is linked to the respective differential solubility of oxide compounds  
 118 in water. This hypothesis is also supported by the fact that a  $\text{Se}^0$  contribution is visible after  
 119 **one-week** ageing (Figure 1 f.), growing up with time. For II-VI materials, the oxidation is a  
 120 two-step process, with in a first time, the appearance of  $\text{Se}^0$  contribution which act as an  
 121 corrosion intermediate and, in a second time, the oxide growth.<sup>13</sup> We proved before that the Se  
 122 ageing mechanism for CIGS surface follow this **II-VI's** scheme.<sup>6,11</sup> An explanation to the fact  
 123 that no Ga, Cu or Se oxide are found, is, in a first time, that CIGS surface undergoes as a  
 124 spontaneous anodic dissolution mechanism in water environment and, in a second time, **that**  
 125 differential dissolution of these oxides occurs.

126

### 127 3.2. Immersion of aged CIGS surfaces

128 To evaluate the solubility of the different oxides present on CIGS surface, aged CIGS samples  
129 (at ambient atmosphere), then covered by all the possible oxide phases, were also immersed in  
130 deionized water (1 hour, 1 day and 1 week) and their surface evolution checked by XPS  
131 measurements (Figure 2). Based on Pourbaix's diagram,<sup>14</sup> InO<sub>x</sub> dissolution in pure water is low  
132 even practically non-existent with a minimum solubility (10<sup>-9.8</sup> g-ion L<sup>-1</sup>). GaO<sub>x</sub> dissolution is  
133 slow but happens in pure water or dilute mineral acids and CuO<sub>x</sub> and SeO<sub>x</sub> dissolutions are  
134 expected to be faster.



135

136 **Figure 2: Normalized evolution of high energy XPS spectra of aged CIGS surface (HCl + KCN treated) over different**  
137 **immersion times in deionized water: GaLMM (a.), CuLMM (b.), SeLMM (c.), InMNN (d.) Auger regions and O1s (e.)**  
138 **and Se3d (f.) photopeaks. The differences observed are represented with an arrow.**

139

140 After one hour immersion, the Cu oxide contribution fully disappears (Figure 2 b.) as well as  
141 the Na initially present on aged surface (Figure 2 d.). Moreover, a decrease of Se oxide Auger  
142 feature is observed (Figure 2 c.), in agreement with the disappearance of the oxide contribution  
143 in the Se3d spectral window (Figure 2 f.). After one day immersion, the entire  $\text{SeO}_x$  contribution  
144 has disappeared. Concerning Ga, peak ratios between CIGS and oxide contributions (Figure 2  
145 a.) progressively reverse in favor of the CIGS environment. After **one-week** immersion, **Cu and**  
146 **Se** oxides have totally disappeared and the surface presents  $\text{In}_{\text{ox}}$ , residual  $\text{Ga}_{\text{ox}}$  and  $\text{Se}^0$  (Figure  
147 2 d. and e.) All these evolutions are correlated with the decrease of the O1s oxide contribution  
148 at  $531.0 \pm 0.1$  eV (BE) (Figure 2 e.). As expected, the In oxide contribution doesn't present any  
149 evolution over water immersion (Figure 2 d.). Finally, this experiment informs about the  
150 dissolution kinetics of the surface oxide layer on aged CIGS sample:  $\text{Cu}_{\text{ox}} > \text{Se}_{\text{ox}} > \text{Ga}_{\text{ox}}$ ,  $\text{In}_{\text{ox}}$   
151 being almost insoluble.

152

### 153 3.3. ICP-OES measurements

154 Dissolution of Se, Cu and Ga oxides in water was **evidenced** for CIGS surfaces. Study was **thus**  
155 **completed with** the dosage of the water solutions in which CIGS samples were immersed using  
156 ICP-OES (Table 2). Considering the amounts measured in the different solutions, the  
157 dissolution of Se, Cu and Ga is demonstrated, with different kinetics consistent with the oxide  
158 solubilities presented in the previous paragraph. Cu is the first element detected by ICP-OES  
159 indicating that  $\text{Cu}_{\text{ox}}$  dissolution occurs in a short timescale, after one week of ageing in water.  
160 The global balance between oxide formation and dissolution leads to CGI value increase. After  
161 one week, only traces are detected in solution and the Cu surface enrichment progressively  
162 continues to increase (Table 1). Se and Ga traces appear in solution only after 2 and 3 weeks of  
163 ageing in water respectively, in good agreement with previous observations on aged surface  
164 evolution in water, with no traces of  $\text{Se}_{\text{ox}}$  neither  $\text{Ga}_{\text{ox}}$ .

165 Concerning Na, a really high concentration is measured even after one week. To determine the  
166 contribution of the glass substrate from the sides not covered by CIGS and correct the amount  
167 of Na detected only by migration through the absorber layer, samples presenting the same  
168 dimension but consisting in glass covered with Mo only have been immersed in water. From  
169 this experiment, the Na concentration in water solution per week measured is  $200 \mu\text{g L}^{-1}$ . The  
170 CIGS deposited on top of Mo acts thus as a pump for sodium and releases Na.



171

#### 172 **4. Conclusion**

173 In aqueous media, CIGS surface presents many chemical evolutions. Each CIGS constitutive  
174 element presents its own oxidation kinetic as well as its own dissolution kinetic in water, leading  
175 to a drastic disorganization of the CIGS network. The resulting surface is representative of  
176 several environments: the CIGS one and the oxidized one. However, some of the oxides  
177 dissolve directly inside water due to their solubilities. Two specific features are observed for  
178 the elements of column III, as  $\text{In}_{\text{ox}}$  grows rapidly and remains stable in time, without  
179 dissolution (in coherence with Pourbaix's diagram) while the oxidized contribution of Ga  
180 appears with a slower kinetic, as well as its dissolution. Regarding Se behavior, spontaneous  
181 oxidation and dissolution at open-circuit potential in water are noticed and supported by the  
182 presence of the corrosion intermediate  $\text{Se}^0$ . Evolution of Cu is similar to the Se one, leading to  
183 a migration of Cu towards the CIGS surface, in contradiction with the trends observed during  
184 ageing at ambient atmosphere. This disorganization is accompanied with a major dissolution of  
185 Na, coming from the CIGS bulk as well as a surface delamination over time.

#### 186 **Acknowledgments**

187 The authors thank Wolfram Hempel from ZSW, Germany and Sofia Gaiaschi and Patrick  
188 Chapon from Horiba Scientific for CIGS samples supply. This work has been carried out in the  
189 framework of the project I of IPVF (Institut Photovoltaïque d'Ile-de-France). This project has  
190 been supported by the French Government in the frame of the program "Programme  
191 d'Investissement d'Avenir—ANR-IEED-002-01."

#### 192 **References**

- 193 1. Nakamura M, Yamaguchi K, Kimoto Y, Yasaki Y, Kato T, Sugimoto H. Cd-free Cu  
194  $(\text{In,Ga})(\text{Se,S})_2$  thin film solar cell with a new world record efficacy of 23.35%. *IEEE J*  
195 *Photovoltaics* . 2019:1-5. doi:10.1109/JPHOTOV.2019.2937218
- 196 2. Theelen M, Foster C, Steijvers H, Barreau N, Vroon Z, Zeman M. The impact of  
197 atmospheric species on the degradation of CIGS solar cells. *Sol Energy Mater Sol*  
198 *Cells*. 2015. doi:10.1016/j.solmat.2015.05.019
- 199 3. Theelen M, Dasgupta S, Vroon Z, et al. Influence of the atmospheric species water,  
200 oxygen, nitrogen and carbon dioxide on the degradation of aluminum doped zinc oxide

- 201 layers. *Thin Solid Films*. 2014;565:149-154. doi:10.1016/J.TSF.2014.07.005
- 202 4. Theelen M. Impact of atmospheric species on copper indium gallium selenide solar cell  
203 stability: an overview. *J Photonics Energy*. 2016;6(1):015501.  
204 doi:10.1117/1.JPE.6.015501
- 205 5. Calvet W, Ümsür B, Steigert A, et al. *In situ* investigation of as grown Cu(In,Ga)Se<sub>2</sub>  
206 thin films by means of photoemission spectroscopy. *J Vac Sci Technol A*.  
207 2019;37(3):031510. doi:10.1116/1.5089412
- 208 6. Loubat A, Béchu S, Bouttemy M, et al. Cu depletion on Cu(In,Ga)Se<sub>2</sub> surfaces  
209 investigated by chemical engineering: An x-ray photoelectron spectroscopy approach. *J*  
210 *Vac Sci Technol A*. 2019;37(4):041201. doi:10.1116/1.5097353
- 211 7. Loubat A, Eypert C, Mollica F, et al. Optical properties of ultrathin CIGS films studied  
212 by spectroscopic ellipsometry assisted by chemical engineering. *Appl Surf Sci*.  
213 2017;421:643-650. doi:10.1016/j.apsusc.2016.10.037
- 214 8. Lehmann J, Lehmann S, Lauer mann I, et al. Reliable wet-chemical cleaning of natively  
215 oxidized high-efficiency Cu(In,Ga)Se<sub>2</sub> thin-film solar cell absorbers. *J Appl Phys*.  
216 2014;116(23):233502. doi:10.1063/1.4903976
- 217 9. Dimmler B, Schock HW. Scaling-up of CIS technology for thin-film solar modules.  
218 *Prog Photovoltaics Res Appl*. 1996;4(6):425-433. doi:10.1002/(SICI)1099-  
219 159X(199611/12)4:6<425::AID-PIP153>3.0.CO;2-Y
- 220 10. Skoog DA, West DM, Hollar JF. Fundamentals of Analytical Chemistry. Sixth edition.  
221 *J Chem Educ*. 1992;69(11):A305. doi:10.1021/ed069pA305.1
- 222 11. Canava B, Vigneron J, Etcheberry A, Guillemoles J., Lincot D. High resolution XPS  
223 studies of Se chemistry of a Cu(In, Ga)Se<sub>2</sub> surface. *Appl Surf Sci*. 2002;202(1-2):8-14.  
224 doi:10.1016/S0169-4332(02)00186-1
- 225 12. Hedström J, Ohlsen H, Bodegård M, et al. ZnO/CdS/Cu(In,Ga)Se<sub>2</sub> thin film solar cells  
226 with improved performance. In: *Proceedings of the 23rd IEEE Photovoltaic*  
227 *Specialists* . Louisville, KY, USA: The Institute of Electrical and Electronics  
228 Engineers, Inc; 1993:364-371.
- 229 13. Chassaing E, Grand P-P, Ramdani O, Vigneron J, Etcheberry A, Lincot D.

- 230            Electrocrystallization Mechanism of Cu–In–Se Compounds for Solar Cell  
231            Applications. *J Electrochem Soc.* 2010;157(7):387-395. doi:10.1149/1.3374590
- 232    14.    Pourbaix M. *Atlas d'Equilibres Electrochimiques*. Paris: Gauthier-Vilars; 1963.
- 233

234 **Table 1: GGI and CGI ratios evolution of CIGS surfaces aged in H<sub>2</sub>O environment, calculated from the Ga2p<sub>3/2</sub>, Cu2p<sub>3/2</sub>**  
235 **and In3d<sub>5/2</sub> regions after HCl + KCN chemical treatment.**

	GGI	CGI
t <sub>0</sub>	0.28 ± 0.03	0.98 ± 0.05
1 week	0.15 ± 0.03	3.09 ± 0.05
2 weeks	0.14 ± 0.03	3.14 ± 0.05
3 weeks	0.14 ± 0.03	3.21 ± 0.05
4 weeks	0.14 ± 0.03	3.49 ± 0.05

236

237

238

239 **Table 2: Evolution of element concentrations in aged waters measured by ICP-OES for a “reference” CIGS surface. Na**  
240 **value is not corrected.**

	Concentration ( $\mu\text{g L}^{-1}$ ) $\pm 10 \mu\text{g L}^{-1}$				
Ageing time	Cu	Ga	In	Se	Na
1 week	236	/	/	/	641
2 weeks	264	/	/	161	1459
3 weeks	269	33	/	316	2480
4 weeks	278	118	/	355	2658

241